The End-to-End Performance of Rateless Codes in Poisson Bipolar and Cellular Networks

Na Deng, *Member, IEEE*, and Martin Haenggi, *Fellow, IEEE*

***Abstract*—Rateless coding is a promising forward error correction technique to meet both delay and reliability requirements of emerging wireless applications. However, existing works on rateless codes mostly considered finite networks or ignored the traffic dynamics. In this paper, we present a comprehensive investigation of the end-to-end performance for rateless codes in Poisson bipolar and cellular networks. Specifically, we propose the notion of the *end-to-end success probability*, which is the success probability given an end-to-end delay requirement, to jointly evaluate the delay performance and transmission reliability of rateless codes. To fully characterize the end-to-end delay, we divide it into two parts, namely the packet waiting time and the transmission time, and provide tractable yet accurate approximations to their statistical distributions. Compared with the previous works, the proposed general framework and the end-to-end performance metric help obtain insights on the role of scheduling, queueing, and coding scheme in practical radio access networks. The approximations are verified to be effective and reliable through simulations. Overall, the results show the significant benefits of rateless codes relative to the fixed-rate codes in terms of the transmission reliability with an end-to-end delay requirement.**

***Index Terms*—Rateless codes, end-to-end delay, reliability, stochastic geometry, queueing theory, packet waiting and transmission time.**

I. Introduction

A. Motivation

With the rapid development of the mobile Internet, Internet of Things and smart terminals, the fifth-generation (5G) mobile network and beyond face a variety of latency-critical applications, such as intelligent manufacturing, remote control, auxiliary driving, and automatic driving, that lead to stringent end-to-end delay and reliability requirements [2]. Generally, the end-to-end delay consists of two main parts: one is the queueing delay, which is the waiting time until transmission starts [3]; the other is the transmission delay[1]. Due to the unprecedented data volumes and heavy traffic load in current communication systems, buffers are usually used at transceivers such that the queueing delay plays an increasingly critical role in the end-to-end delay performance.

Delay and reliability are two commonly used performance metrics in the analysis and design of wireless networks, which rely on and influence each other [5]. In particular, the end-to-end delay can be reduced through the improvement of the signal-to-interference ratio (SIR). For a single transmission, links with higher SIR usually have higher transmission reliability, leading to lower transmission delay. Meanwhile, when a retransmission mechanism is applied, links with higher transmission reliability also reduce the number of retries and the backlog of packets. Accordingly, both the transmission delay and the queueing delay are reduced. Therefore, transmission reliability has become increasingly dominant in affecting the diverse performance requirements of 5G wireless networks.

To improve the transmission reliability, forward error correction (FEC) is one of the most effective and commonly used techniques for data transmission over unreliable or noisy communication channels. Recently, rateless codes have received widespread attentions as a promising FEC technique, with the goal of reducing the transmission delay while improving the transmission reliability and throughput [6–9]. Compared with fixed-rate codes, rateless codes adapt both the code construction and the number of parity symbols to time-varying channel conditions and hence complete the transmission of fixed-length information packets faster. More importantly, once the receiver decodes the data, the transmitter stops interfering with other ongoing transmissions, thus the interference in the network can be substantially mitigated. Accordingly, as an effective FEC coding approach, rateless codes are expected to cope with both the reliability and delay requirements of emerging applications.

While there have been many studies on the seamless integration of rateless codes into wireless networks in recent years, the impacts of the queueing process on the end-to-end delay and reliability performance of rateless codes have not been explored in depth. Furthermore, since delay is an intricate function of all links and affected by a variety of factors such as the temporal variation of traffic, the medium access protocol, the spatial distribution of transceivers, etc., the theoretical analysis of the delay in large-scale wireless networks is still challenging but imperative to guide the practical design and operation. Thus, our paper focuses on the end-to-end delay and reliability performance of rateless codes in large-scale networks, taking the random arrival and queueing of packets at the terminals into account.

Na Deng is with the School of Information and Communication Engineering, Dalian University of Technology (DLUT), Dalian, 116024, China, and also with the National Mobile Communications Research Laboratory, Southeast University, Nanjing, 210096, China (e-mail: dengna@dlut.edu.cn). Martin Haenggi is with the Dept. of Electrical Engineering, University of Notre Dame, Notre Dame 46556, USA (e-mail: mhaenggi@nd.edu).

Part of this work has been presented at the 2019 IEEE International Conference on Communications (ICC'19) [1].

This work was supported by the National Natural Science Foundation of China under Grant 61701071, by the China Postdoctoral Science Foundation (2017M621129 and 2019T120204), by the open research fund of National Mobile Communications Research Laboratory, Southeast University (No. 2019D03), by the Fundamental Research Funds for the Central Universities (DUT19RC(4)014), and by the US NSF grant CCF 1525904.

[1]The processing delay and the propagation delay are negligible compared to the queueing delay and the transmission delay [4].

B. Related Work

The conventional delay analysis is usually based on queueing theory with a collision model to simplify the physical layer. However, in practical networks, the effect of the interference cannot be accurately modeled merely by a collision since it is related to the channel fluctuations, path loss, as well as the spatial distribution of the network transceivers. Stochastic geometry has been widely used to characterize the interference in large-scale wireless networks for key performance analysis such as outage probability, average achievable rate, and so on [10–12]. Most of the works in the literature assume saturation conditions for the traffic (i.e., buffers of all network nodes are always full), and thus no insights regarding the end-to-end packet delay can be obtained since the queueing dynamics are ignored. Accordingly, integrating the queueing dynamics into the stochastic geometry-based model is a promising way to accurately analyze the end-to-end delay performance. In this line of research, the delay performance was analyzed for Poisson ad hoc networks [13] and TDMA/ALOHA multihop networks in a Poisson field of interference [14]. In [15], the authors proposed a tractable approach to analyze the delay in heterogenous cellular networks with spatio-temporal random arrival of traffic. However, they focused on the delay performance with retransmission when the received SINR is less than a predefined threshold and used the mean queueing delay to measure the end-to-end delay performance with the adoption of fixed-rate codes.

Since rateless coding was firstly applied and analyzed in a two-hop network with parallel relays [16], it has received a widespread attention in the fields of sensor networks [17], cellular networks [18], underwater acoustic networks [19], wireless information and energy transfer networks [20]. Though the benefits of the rateless codes in terms of many performance metrics such as delay, reliability, throughput, etc., have been investigated, these works only focus on wireless networks with a finite number of elements. While the authors in [21] and [22] extended the performance analysis of rateless codes to large-scale ad hoc and cellular networks using tools from stochastic geometry, the full-buffer assumption (i.e., transmitters in the network always have packets to transmit), which neglects the queueing dynamics, leads to significant deviations from the actual end-to-end delay performance. In summary, there is so far no comprehensive investigation of the end-to-end performance of rateless codes in large-scale wireless networks considering the impact of the queueing process. We will fill this gap with new analytical results for the end-to-end delay and reliability performance with rateless codes and buffers at transmitters.

C. Contributions

Combining the tools from stochastic geometry and queueing theory, we characterize the end-to-end performance of rateless codes in radio access networks, where the spatial distribution and the spatio-temporal traffic of transmitters follow a homogeneous Poisson point process (PPP) [12] and a Poisson arrival process (PAP), respectively. The end-to-end delay is divided into two parts: the packet waiting time and the transmission time, where the former is presented by an M/Geo/1 queueing model [23] with random scheduling and the latter corresponds to the decoding time of rateless coding for a packet with fixed-size information.

Specifically, we first provide an exact statistical distribution of the packet waiting time and propose an accurate approximation via the concept of effective bandwidth [24, 25] to facilitate the further analysis. The results reveal that the logarithm of the distribution of the packet waiting time decays linearly with time. For the analysis of the packet transmission delay, we propose three approaches to bound or approximate its statistical distribution by simplifying the behavior of the interference in Poisson bipolar and cellular networks. Interestingly, it turns out that the distribution of the packet transmission time is not affected by the scheduling probability as long as the arrival rate is smaller than the service rate. Since the packet waiting time and the packet transmission time are interdependent given an end-to-end delay requirement, we further quantify the end-to-end success probability—the probability of a successful transmission within an end-to-end delay constraint—of rateless codes to reflect the impact of such mutual influence on the delay and reliability characteristics jointly. As a benchmark, the end-to-end success probability of fixed-rate codes in each type of network is also derived. Numerical results validate that among the three proposed approximations, the independent-interferer approximation most accurately matches the actual packet transmission time. Moreover, the impacts of some key parameters, such as the scheduling probability, network density, path loss exponent, and frame duration on the end-to-end success probability are investigated numerically, and the results demonstrate the prominent advantage of rateless codes over fixed-rate codes.

In summary, the theoretical results lead to general insights into how the delay and reliability performance of rateless codes are impacted by system design parameters and propagation effects as well as their intricate relationships, while either eliminating the need for extremely time-consuming simulations completely or drastically reducing the ranges of the simulation parameters.

II. System Model

A. Network Model

We employ rateless codes for the information transmissions in interference-limited networks, where the (potential) transmitters form a homogeneous PPP Φ of density λ with unit transmit power. We consider the typical receiver at the origin that attempts to receive a signal from a transmitter. This model comprises both bipolar and cellular networks, and the difference lies in how the desired transmitter is chosen. According to the concept of the frame (or subframe) in 4G and future 5G networks [26], the time domain is divided into discrete frames with equal duration T_{f}. We use the standard path loss model with exponent α, where $\ell(x) = |x|^{-\alpha}$ represents the path loss function between transmitter x and the origin. The power fading coefficient associated with transmitter x in frame k is denoted by $h_{x,k}$, which is assumed to be an exponential random variable with $\mathbb{E}(h_{x,k}) = 1$ (Rayleigh fading). In

addition, the fading coefficients remain constant over each frame and are spatially and temporally independent.

Each transmitter has a buffer of infinite capacity to store the generated packets and to apply the first-input-first-output (FIFO) rule to transmit packets. The packets at each transmitter are generated according to a PAP with arrival rate ζ (packets per second), and each packet has K information bits. The arrival processes at different transmitters are independent of each other. Specifically, at the beginning of each frame, each node in Φ independently attempts to send its head-of-line packet with probability p if its buffer is not empty (i.e., it uses ALOHA[2]). During each transmission, K information bits are encoded by a rateless code and sent via Gaussian symbols incrementally over the channel. At the receiver side, the channel output symbols are collected to decode the K information bits with the corresponding rateless decoder. The transmission of the parity symbols continues until the receiver succeeds decoding the K information bits and sends an acknowledgment (ACK) signal[3] to the transmitter or the frame runs out. Due to the inherent property of the rateless code, we assume no retransmission mechanism since it would be more sensible to continue the rateless transmission rather than re-transmitting (from scratch), which is an essential difference from the commonly used fixed-rate codes. When the typical receiver is receiving signals from its transmitter, all the other active transmitters are interferers until their transmissions are completed. In other words, once the interferers receive the ACK from their corresponding receivers, they become silent and stop interfering with other ongoing transmissions.

B. Delay Characterization

The end-to-end delay of packet transmission is evaluated in two phases: one is the waiting phase where the packet waiting time measures the delay between the time when a packet arrives at the buffer and the time when it starts to be transmitted; the other is the transmission phase where the packet transmission time is either the time to successfully transmit a packet within a frame or the frame duration.

1) Packet Waiting Time: Due to the PAP of the packets and the ALOHA scheme, an M/Geo/1 queueing model with arrival rate ζ is adopted to characterize the queueing process at each transmitter. Its service time T_{sv} follows a geometric distribution as

$$\mathbb{P}(T_{\mathrm{sv}} = nT_{\mathrm{f}}) = (1-p)^{n-1}p,\ n \geq 1. \tag{1}$$

Then the statistics of the sojourn time T_{sj} of a packet in the M/Geo/1 queue can be obtained by those of T_{sv} and the Pollaczek-Khinchine transform equation [23], which will be given in the next section. Denote by T_{w} the waiting time for a given packet. Since each packet is transmitted from the start of each frame and the transmission time does not exceed the current frame duration, the packet waiting time is $T_{\mathrm{w}} = T_{\mathrm{sj}} - T_{\mathrm{f}}$.

[2]In cellular networks, we use the ALOHA mechanism to model the activity of each base station caused by load distributions, the scheduling and muting strategies.

[3]The feedback message is usually transmitted via a dedicated channel, separate of the data transmission [26].

2) Packet Transmission Time: Thanks to the adoption of rateless codes, the packet transmission time is less than the frame duration if the packet is transmitted successfully. For $k \in \mathbb{N}$, let t_k be the starting time of the k-th frame, i.e., $t_k = kT_{\mathrm{f}}$. Denoting by x_0 the transmitter corresponding to the typical receiver and $\Phi' = \Phi \setminus \{x_0\}$, the instantaneous interference at the typical receiver at time t in frame k is

$$I_k(t) = \sum_{x \in \Phi'} \ell(x) h_{x,k} B_{x,k} \mathbf{1}_{Q_{x,k}>0} e_{x,k}(t), \quad t_k \leq t < t_{k+1}, \tag{2}$$

where the subscripts k and x denote the k-th frame and transmitter x, respectively, $Q_{x,k}$ is the number of packets in the queue of transmitter x, $B_{x,k} \in \{0,1\}$ denotes whether x attempts to transmit data in frame k and $B_{x,k} = 1$ with probability p, $e_{x,k}(t) = \mathbf{1}(t_k \leq t \leq t_k + T_{x,k})$ denotes the active state of transmitter x at time t, and $T_{x,k}$ is the packet transmission time between the transmitter x and its receiver. We assume that the receiver employs a nearest-neighbor decoder to perform minimum Euclidean distance decoding merely based on the desired channel gain, as suggested in [27]. Thus the achievable rate[4] $C_k(t)$ is

$$C_k(t) = W \log_2(1 + \hat{\mathrm{SIR}}(t)), \tag{3}$$

where W denotes the bandwidth for information transmission, $\hat{\mathrm{SIR}}(t) = \ell(x_0)h_{x_0,k}/\hat{I}_k(t)$ is the time-average received SIR, and $\hat{I}_k(t)$ represents the time-average interference at the typical receiver from t_k up to time t, given by

$$\begin{aligned}\hat{I}_k(t) &= \frac{1}{t-t_k}\int_{t_k}^{t} I_k(\tau)\mathrm{d}\tau \\ &= \sum_{x \in \Phi'} \ell(x) h_{x,k} B_{x,k} \mathbf{1}_{Q_{x,k}>0} \eta_{x,k}(t), \quad t_k \leq t < t_{k+1},\end{aligned} \tag{4}$$

where

$$\eta_{x,k}(t) = \frac{1}{t-t_k}\int_{t_k}^{t} e_{x,k}(\tau)\mathrm{d}\tau = \min\left\{1, \frac{T_{x,k}}{t-t_k}\right\}. \tag{5}$$

Since each interfering transmitter ceases to interfere with other ongoing transmissions after receiving the ACK signal, $\hat{I}_k(t)$ is a monotonically decreasing function of t within each frame, and thus $C_k(t)$ is monotonically increasing with t. Letting $\hat{T}_k$ be the time needed to decode a packet with K information bits in frame k, we have

$$\hat{T}_k = \min\{t : K < t \cdot C_k(t)\}, \tag{6}$$

and the packet transmission time follows as $T_k = \min\{\hat{T}_k, T_{\mathrm{f}}\}$.

III. Delay Analysis

In this section, we first give an exact analytical expression and a simple approximation for the complementary cumulative distribution function (CCDF) of the packet waiting time. Second, we provide three approaches to bound or approximate the CCDF of the packet transmission time by simplifying the behavior of the interferers.

[4]Note that with finite block length, there is a gap to the Shannon limit [28]. However, since the gap affects both the fixed-rate and rateless codes, we use the Shannon limit as a benchmark to highlight the advantage of rateless codes in terms of the end-to-end performance relative to fixed-rate codes.

A. Packet Waiting Time Analysis

As mentioned above, $T_{\rm w} = T_{\rm sj} - T_{\rm f}$, hence $\mathbb{P}(T_{\rm w} > b) = \mathbb{P}(T_{\rm sj} > b + T_{\rm f})$, and we derive the CCDF for $T_{\rm sj}$ using standard queueing theory. According to the Pollaczek-Khinchine transform equation for the sojourn time [23, Eq. 5.13], the Laplace-Stieltjes transform (LST)[5] of $T_{\rm sj}$ is

$$\mathcal{L}_{T_{\rm sj}}(s) = \frac{(1-\varepsilon)s\mathcal{L}_{T_{\rm sv}}(s)}{s - \zeta[1 - \mathcal{L}_{T_{\rm sv}}(s)]}, \tag{7}$$

where $\varepsilon = \zeta T_{\rm f}/p$ (where $\varepsilon < 1$ is assumed to guarantee a finite queueing delay) is the probability that the buffer is not empty and

$$\mathcal{L}_{T_{\rm sv}}(s) = \sum_{n=1}^{\infty}(1-p)^{n-1}pe^{-snT_{\rm f}} = \frac{pe^{-sT_{\rm f}}}{1-(1-p)e^{-sT_{\rm f}}} \tag{8}$$

is the LST of $T_{\rm sv}$. Through the inverse transform, the CCDF of the packet waiting time is

$$\mathbb{P}(T_{\rm w} > b) = 1 - \frac{1}{2\pi j}\int_{\gamma-j\infty}^{\gamma+j\infty}\frac{\exp(s(b+T_{\rm f}))}{s}\mathcal{L}_{T_{\rm sj}}(s){\rm d}s, \tag{9}$$

where $j = \sqrt{-1}$ and γ is a real number so that the path of integration is in the region of convergence (ROC) of $\mathcal{L}_{T_{\rm sj}}(s)$. Since $T_{\rm sj}$ is non-negative, the ROC is ${\rm Re}\{s\} > {\rm Re}\{P_0\}$, where P_0 is the solution of the equation $\exp(-sT_{\rm f}) = \frac{s-\zeta}{(1-p)s-\zeta}$ of $s \in \mathbb{C}$ with the maximum real part, which can be found by numerical approaches. Since $s = 0$ is always a solution, the ROC is at most ${\rm Re}\{s\} > 0$.

Although (9) can be evaluated by numerical integration, it requires a careful selection of γ, the range of the numerical integration, which depends on the rate of convergence of the integrand, and its step size. Moreover, the results are complicated and provide little insight, which imposes restrictions on further analysis. Therefore, in the following, we provide an approximation to simplify the exact result by means of the effective bandwidth [24, 25].

Theorem 1. *The CCDF of the packet waiting time is approximated by*

$$\mathbb{P}(T_{\rm w} > b) \approx \frac{\zeta T_{\rm f}}{p}\exp\Big(-\zeta(e^{u^*}-1)(b+T_{\rm f}) + u^*\Big), \quad b > 0, \tag{10}$$

where $u^* > 0$ satisfies

$$\zeta(e^{u^*}-1) + \frac{1}{T_{\rm f}}\log\left(pe^{-u^*} + 1 - p\right) = 0. \tag{11}$$

Moreover,

$$\mathbb{P}(T_{\rm w} = 0) \approx 1 - \frac{\zeta T_{\rm f}}{p}e^{-\zeta(\exp(u^*)-1)T_{\rm f}+u^*}. \tag{12}$$

Proof: See Appendix A.

[5]Letting $F_X(x)$ be the cumulative distribution function (CDF) of the random variable X, $\mathcal{L}_X(s)$ denotes the LST of X i.e., $\mathcal{L}_X(s) = \int_0^\infty e^{-sx}{\rm d}F_X(x)$. If F has a derivative f, the LST of X is the standard Laplace transform.

Note that $\mathbb{P}(T_{\rm w} = 0)$ represents the probability that a packet arrives at an empty queue and thus is transmitted immediately[6]. Letting $\mathcal{W}(x)$ be the Lambert W function, which solves $\mathcal{W}(x)e^{\mathcal{W}(x)} = x$, we have $u^* = -\zeta T_{\rm f} - \mathcal{W}\big(-\zeta T_{\rm f}e^{-\zeta T_{\rm f}}\big)$ when $p = 1$. For $p < 1$, from Thm. 1, u^* can be obtained by solving the equation in (11) via numerical techniques. The numerical approach usually requires setting an initial range, which is provided in the following corollary. It also establishes the uniqueness of the solution of (11).

Corollary 1. *Letting*

$$u_{\rm u} = \frac{1}{\zeta}\Big(-\zeta + 1/T_{\rm f} + \sqrt{(\zeta - 1/T_{\rm f})^2 - 2\zeta\log(p)/T_{\rm f}}\Big),$$
$$u_{\rm l} = \log\Big(\frac{-p + \sqrt{p^2 - 4(1-p)p/(\zeta T_{\rm f})}}{2(1-p)}\Big), \tag{13}$$

the solution of (11) is unique and lies in $(u_{\rm l}, u_{\rm u})$ for $p < 1$.

Proof: Letting $f(u) = \zeta(e^u - 1) + \frac{1}{T_{\rm f}}\log\left(pe^{-u} + 1 - p\right)$, we have $f(0) = 0$, and its first-order derivative is

$$f'(u) = \zeta e^u\Big(1 - \frac{p}{\zeta T_{\rm f}}\frac{1}{pe^u + (1-p)e^{2u}}\Big), \tag{14}$$

which changes from negative to positive as u increases. Accordingly, it means that $f(u)$ decreases at first and increases later, and thus the solution of $f(u) = 0$ is unique for $u > 0$. From the monotonicity of $f(u)$, u^* is larger than the solution of $f'(u) = 0$, and we have a lower bound of u^* as

$$u_{\rm l} = \log\Big(\frac{-p + \sqrt{p^2 - 4(1-p)p/(\zeta T_{\rm f})}}{2(1-p)}\Big). \tag{15}$$

As for an upper bound $u_{\rm u}$ of u^*, we first obtain

$$f(u) > \zeta(u + u^2/2) + \frac{1}{T_{\rm f}}\log(pe^{-u}) = g(u), \tag{16}$$

and $u_{\rm u}$ is the solution of $g(u) = 0$, given by

$$u_{\rm u} = \frac{-(\zeta - 1/T_{\rm f}) + \sqrt{(\zeta - 1/T_{\rm f})^2 - 2\zeta\log(p)/T_{\rm f}}}{\zeta}. \tag{17}$$

■

B. Packet Transmission Time Analysis

Since each transmitter attempts to transmit independently at the beginning of each frame, the achievable rate and the packet transmission time are statistically identical in each frame. Thus, the frame index can be omitted. To characterize the CCDF of the packet transmission time, we note that T and $\hat{T}$ are related as

$$\mathbb{P}(T > b) = \begin{cases} \mathbb{P}(\hat{T} > b) & b \le T_{\rm f} \\ 0 & b > T_{\rm f}. \end{cases} \tag{18}$$

According to (6), we have

$$\mathbb{P}(\hat{T} > b) = \mathbb{P}\big(K > b \cdot C(b)\big) = \mathbb{P}\left(K > bW\log_2\left(1 + \frac{\ell(x_0)h_{x_0}}{\hat{I}(b)}\right)\right)$$

[6]In this case, to facilitate the analysis, the waiting time before the next frame starts is neglected due to the adoption of the M/Geo/1 model, in other words, the packet waiting time in this case is approximated to be zero.

$$= 1-\mathbb{P}\Big(\frac{\ell(x_0)h_{x_0}}{\hat{I}(b)} > \theta_b\Big)$$
$$\overset{(a)}{=} 1-\mathbb{E}\Big[\exp\big(-\theta_b r_0^{\alpha}\hat{I}(b)\big)\Big]$$
$$= 1-\mathbb{E}_{r_0}\Big[\mathcal{L}_{\hat{I}(b)}(\theta_b r_0^{\alpha} \mid r_0)\Big], \tag{19}$$

where step (a) follows since h_{x_0} is an exponential distributed variable, $\theta_b = 2^{\frac{K}{bW}} - 1$, $r_0 = |x_0|$ and $\mathcal{L}_X(s) = \mathbb{E}_X(\exp(-sX))$ is the Laplace transform of the random variable X. Eq. (19) implies that the CCDF of the packet transmission time is related to two factors: one is the distance r_0 between the typical receiver and its corresponding transmitter; the other is the Laplace transform of $\hat{I}(b)$, which is determined by the spatial distribution of the interfering transmitters Φ', and both depend on how the receiver chooses its transmitter. In the following two sections, we analyze the specific cases of Poisson bipolar and cellular networks.

It should be noted that for the packet transmission time analysis, the main technical difficulty lies in the interaction between the interference and the actual transmission time of rateless codes. To be specific, whether the interference is strong or weak largely depends on the number and position of concurrent transmitters, and whether a transmitter is active or not depends on the actual time for a successful transmission of rateless codes, which, in turn, is directly influenced by the interference. Thus, a direct calculation of the exact CCDF of the packet transmission time seems infeasible and we turn to giving bounds or approximations for the analytical result via the following three approaches [22] to simplify the behavior of the interferers.

- **Dummy-interferer bound (DIB)**: Consider a dummy-interferer system in which the interfering transmitters continue to transmit "dummy" signals and interfere with other ongoing transmissions even after they have received the ACK from the receivers. Therefore, the transmitters causing interference at the typical receiver remain constant in this system, and the resulting packet transmission time will be larger than the actual one.
- **Nearest-interferer approximation (NIA)**: Consider a nearest-interferer system in which only the nearest interfering transmitter is active during the entire frame and the interference from other interfering transmitters is ignored. The rationale behind this approximation is that the interference from the nearest interferer usually dominates the total interference (at least when the path loss exponent is not small) and hence the packet transmission for the typical receiver.
- **Independent-interferer approximation (IIA)**: Consider an independent-interferer system in which the packet transmission time $\bar{T}_x$ of each interfering transmitter is statistically independent with an identical CCDF $\mathbb{P}(\bar{T} > b)$. Besides, the CCDF of $\bar{T}_x$ can be taken to be the one for the typical receiver in the dummy-interferer system or the nearest-interferer system, which can be viewed as two extreme cases. Therefore, the interference at the typical receiver in this system is decoupled from the actual packet transmission time, resulting in an approximation.

IV. Poisson Bipolar Networks

In this section, we consider the *Poisson bipolar model* [12, Def. 5.8], where each transmitter is assumed to have a dedicated receiver at a fixed distance r_0 in a random orientation. Due to the conditioning property of the PPP [12, Box 8.2], adding a point at x_0 is the same as conditioning on $x_0 \in \Phi$ in a PPP. Therefore, we consider the transmitter x_0 located at $(r_0, 0)$ to send packets to the typical receiver, and the set of potential interfering transmitters Φ' forms a PPP on the plane. Under this setup, we provide bounds and approximations on the CCDF of the packet transmission time through the three approaches described in Sec. III-B, based on which we can then characterize the end-to-end performance of rateless codes combined with the results related to the packet waiting time.

1) Dummy-interferer bound: In this system, we can upper bound the interference $\hat{I}(t)$ as

$$\hat{I}(t) = \sum_{x\in\Phi'} \ell(x)h_x B_x \mathbf{1}_{Q_x>0}\eta_x(t)$$
$$< \sum_{x\in\Phi'} \ell(x)h_x B_x \mathbf{1}_{Q_x>0} = I_{\mathrm{di}}. \tag{20}$$

Then, the upper bound for the CCDF of T can be obtained by replacing the Laplace transform of $\hat{I}(b)$ in (19) with that of I_{di}, given in the following theorem.

Theorem 2. *Let $\delta \triangleq 2/\alpha$, and*

$$P_{\mathrm{di}}(\theta_b) \triangleq 1-\exp\Big(-\pi\lambda\zeta T_{\mathrm{f}}\Gamma(1+\delta)\Gamma(1-\delta)\theta_b^{\delta}r_0^2\Big). \tag{21}$$

Given that the typical transmitter is active, the CCDF of the packet transmission time for the typical receiver in Poisson bipolar networks is upper bounded as $\mathbb{P}(T > b) < P_{\mathrm{di}}(\theta_b)$, for $b \le T_{\mathrm{f}}$.

Proof: According to (19) and (20), we have

$$\mathbb{P}(\hat{T} > b) = 1-\mathbb{P}\Big(\frac{r_0^{-\alpha}h_{x_0}}{\hat{I}(b)} > \theta_b\Big)$$
$$< 1-\mathbb{P}\Big(\frac{r_0^{-\alpha}h_{x_0}}{I_{\mathrm{di}}} > \theta_b\Big)$$
$$= 1-\mathcal{L}_{I_{\mathrm{di}}}(\theta_b r_0^{\alpha}), \tag{22}$$

where the Laplace transform of I_{di} is [12, Sec. 5.17]

$$\mathcal{L}_{I_{\mathrm{di}}}(s) = \exp\Big(-\pi\lambda p\varepsilon\Gamma(1+\delta)\Gamma(1-\delta)s^{\delta}\Big), \tag{23}$$

and the final result is obtained by inserting (23) in (22). ∎

It should be noted that the arrival rate should be less than the service rate to guarantee a finite queueing delay, i.e., $\varepsilon < 1$. Otherwise, the buffer at each transmitter will never be empty, and hence the upper bound for the CCDF of T becomes

$$\mathbb{P}(T > b) < 1-\exp\Big(-\pi\lambda p\Gamma(1+\delta)\Gamma(1-\delta)\theta_b^{\delta}r_0^2\Big). \tag{24}$$

2) Nearest-interferer approximation: In this system, denoting by x_1 the nearest active interferer for the typical receiver, the achievable rate is obtained by

$$C = W\log_2\left(1+\frac{h_{x_0}\ell(x_0)}{h_{x_1}\ell(x_1)}\right). \tag{25}$$

Theorem 3. *Letting $T_{\rm ni}$ be the packet transmission time of the typical receiver in the nearest-interferer system and given that the typical transmitter is active, we have*

$$\mathbb{P}(T_{\rm ni} > b) = 1 - \int_0^{\infty} \frac{\exp(-r){\rm d}r}{1+\theta_b r_0^{\alpha}(\pi\lambda\zeta T_{\rm f})^{\frac{\alpha}{2}} r^{-\frac{\alpha}{2}}}, \quad b \le T_{\rm f}. \tag{26}$$

Proof: Since each interferer in Φ' sends its packet with probability p in each frame and the probability of a non-empty buffer is ε, the set of active interferers form a PPP by independently thinning Φ' with probability $p\varepsilon$. Thus, the distance between the nearest active interfering transmitter x_1 to the origin has the probability density function (PDF) [29]

$$f_{|x_1|}(r) = 2\pi\lambda p\varepsilon r \exp(-\pi\lambda p\varepsilon r^2). \tag{27}$$

According to (25), we have

$$\begin{aligned}
\mathbb{P}(T_{\rm ni} > b) &= \mathbb{P}\Big(K > bW\log_2\Big(1+\frac{h_{x_0}\ell(x_0)}{h_{x_1}\ell(x_1)}\Big)\Big) \\
&= 1 - \mathbb{P}\Big(\frac{h_{x_0} r_0^{-\alpha}}{h_{x_1}|x_1|^{-\alpha}} > \theta_b\Big) \\
&= 1 - \mathbb{E}\Big[\frac{1}{1+\theta_b r_0^{\alpha}|x_1|^{-\alpha}}\Big] \\
&= 1 - \int_0^{\infty} \frac{f_{|x_1|}(r){\rm d}r}{1+\theta_b r_0^{\alpha} r^{-\alpha}} \\
&= 1 - \int_0^{\infty} \frac{\exp(-r){\rm d}r}{1+\theta_b r_0^{\alpha}(\pi\lambda p\varepsilon)^{\frac{\alpha}{2}} r^{-\frac{\alpha}{2}}}.
\end{aligned} \tag{28}$$

■

3) Independent-interferer approximation: In this system, each interferer starts the packet transmission at the beginning of each frame and continues for a certain duration $\bar{T}_x$, no matter whether the packet is successfully transmitted or not. $\bar{T}_x$ is assumed to be identically independently distributed with the CCDF $\mathbb{P}(\bar{T} > b)$. Thus, the time-average interference at the typical receiver is

$$\bar{I}(t) = \sum_{x\in\Phi'} \ell(x) h_x B_x \mathbf{1}_{Q_x>0} \bar{\eta}_x(t),\ 0 < t \le T_{\rm f}, \tag{29}$$

where $\bar{\eta}_x(t) = \min\{1, \bar{T}_x/t\}$, and the achievable rate follows as

$$C(t) = W\log_2\Big(1+\frac{h_{x_0}\ell(x_0)}{\bar{I}(t)}\Big). \tag{30}$$

Theorem 4. *Let $\mu \triangleq \int_0^{T_{\rm f}} \mathbb{P}(\bar{T} > b){\rm d}b$ be the average packet transmission time of the interfering transmitters in the independent-interferer system. Given that the typical transmitter is active, the CCDF of the packet transmission time $T_{\rm ii}$ in Poisson bipolar networks satisfies*

$$P_{\rm ii}^{\rm l}(\theta_b) \le \mathbb{P}(T_{\rm ii} > b) \le P_{\rm ii}^{\rm u}(\theta_b), \quad b \le T_{\rm f}, \tag{31}$$

where

$$\begin{aligned}
P_{\rm ii}^{\rm u}(\theta_b) \ &= \ 1 - \exp\Big(-\pi\lambda\zeta T_{\rm f}(\min\{1,\frac{\mu}{b}\})^{\delta} \\
&\qquad \times\Gamma(1+\delta)\Gamma(1-\delta)\theta_b^{\delta} r_0^2\Big),
\end{aligned} \tag{32}$$

$$P_{\rm ii}^{\rm l}(\theta_b) \ = \ 1 - \exp\Big(-\pi\lambda\zeta\mu\Gamma(1+\delta)\Gamma(1-\delta)\theta_b^{\delta} r_0^2\Big). \tag{33}$$

Proof: See Appendix B.

From Thm. 4, we can see that the calculation of the CCDF of $T_{\rm ii}$ in the independent-interferer system requires a known CCDF $\mathbb{P}(\bar{T} > b)$ to obtain the average packet transmission time of interfering transmitters μ. A natural choice for such known CCDF is the distribution of the packet transmission time in the dummy- or nearest-interferer system given in Thms. 2 and 3, respectively. Thus, μ can be $\mu_{\rm di}$ or $\mu_{\rm ni}$, given as

$$\mu_{\rm di} = T_{\rm f} - \int_0^{T_{\rm f}} \exp\Big(-\pi\lambda\zeta T_{\rm f}\Gamma(1+\delta)\Gamma(1-\delta)\theta_b^{\delta} r_0^2\Big){\rm d}b, \tag{34}$$

$$\mu_{\rm ni} = T_{\rm f} - \int_0^{T_{\rm f}} \int_0^{\infty} \frac{\exp(-r){\rm d}r{\rm d}b}{1+\theta_b r_0^{\alpha}(\pi\lambda\zeta T_{\rm f})^{\frac{\alpha}{2}} r^{-\frac{\alpha}{2}}}. \tag{35}$$

Remarks: These two options are two extremes and have their own relative merits. Due to the adoption of rateless codes, there are complicated interactions between the packet transmission time for the typical receiver and the interference from other ongoing transmissions. And because of the distance-dependent path loss, such interaction is dominated by the nearby interferers. Therefore, although $\mu_{\rm di}$ has a simpler form, the interference approximated by the dummy-interference system is an overestimation of the real case, and accordingly, it is less accurate than $\mu_{\rm ni}$ for approximating the CCDF of the packet transmission time. As will be shown in Sec. VII-B, the difference between these two options is more evident in cellular networks.

V. Poisson Cellular Networks

In Poisson cellular networks with nearest-base station (BS) association, the distance r_0 between the typical user and its serving BS is random. The PDF of the random variable r_0 is known from [29] as $f_{r_0}(r) = 2\pi\lambda r\exp(-\pi\lambda r^2)$, and the set of potential interfering BSs Φ' forms a PPP outside the circle centered at the origin with the radius r_0. According to (19), the packet transmission time of rateless codes under the cellular network setting follows

$$\mathbb{P}(\hat{T} > b) = 1 - \int_0^{\infty} \mathcal{L}_{\hat{I}(b)}(\theta_b r^{\alpha}) f_{r_0}(r){\rm d}r, \tag{36}$$

and we then use the three approaches proposed in Sec. III-B.

1) Dummy-interferer bound: In this system, the interference $\hat{I}(t)$ in cellular networks is upper bounded by

$$\tilde{I}_{\rm di} = \sum_{x\in\Phi'} \ell(x) h_x B_x \mathbf{1}_{Q_x>0}. \tag{37}$$

Hence, the upper bound for the CCDF of T is obtained through bounding the interference, given in the following theorem.

Theorem 5. *Let $F(\alpha,\theta) \triangleq {}_2F_1(1,-\delta,1-\delta,-\theta_b) - 1$ and*

$$\tilde{P}_{\rm di}(\theta_b) \triangleq 1 - \frac{1}{1+\zeta T_{\rm f} F(\alpha,\theta_b)}, \tag{38}$$

where ${}_2F_1(\cdot)$ is the Gaussian hypergeometric function. Given that the typical BS is active, the CCDF of the packet transmission time for the typical user is upper bounded as $\mathbb{P}(T > b) < \tilde{P}_{\rm di}(\theta_b),\ b \le T_{\rm f}$.

Proof: Given that $r_0 = r$, the Laplace transform of $\tilde{I}_{\rm di}$ in cellular networks evaluated at $s = \theta_b r^\alpha$ is

$$\begin{aligned}\mathcal{L}_{\tilde{I}_{\rm di}}(\theta_b r^\alpha) &= \mathbb{E}\Big[\exp\big(-\theta_b r^\alpha \sum_{x\in\Phi'} \ell(x) h_x B_x \mathbf{1}_{Q_x>0}\big)\Big] \\ &= \mathbb{E}\Big[\prod_{x\in\Phi'}\Big(1-p\varepsilon+p\varepsilon e^{-\theta_b r^\alpha \ell(x) h_x}\Big)\Big] \\ &= \mathbb{E}\Big[\prod_{x\in\Phi'}\Big(1-p\varepsilon+\frac{p\varepsilon}{1+\theta_b r^\alpha |x|^{-\alpha}}\Big)\Big] \\ &\overset{(a)}{=} \exp\Big(-2\pi\lambda p\varepsilon\int_r^\infty\Big(1-\frac{1}{1+\theta_b r^\alpha t^{-\alpha}}\Big)t\mathrm{d}t\Big) \\ &= \exp\Big(-\pi\lambda p\varepsilon r^2\theta_b^\delta\int_{\theta_b^{-\delta}}^\infty\frac{1}{1+t^{\alpha/2}}\mathrm{d}t\Big) \\ &\overset{(b)}{=} \exp\Big(-\pi\lambda p\varepsilon r^2 F(\alpha,\theta_b)\Big), \end{aligned} \tag{39}$$

where step (a) uses the PGFL of the PPP and the integration limit is obtained since the distance between the closest interferer and the typical user is larger than r, and step (b) uses the identity [30]

$$1+\theta^\delta\int_{\theta^{-\delta}}^\infty\frac{1}{1+t^{\alpha/2}}\mathrm{d}t \equiv {}_2F_1(1,-\delta,1-\delta,-\theta). \tag{40}$$

By substituting $\mathcal{L}_{\tilde{I}_{\rm di}}(\theta_b r^\alpha)$ into (36), we obtain

$$\mathbb{P}(\hat{T}>b) < 1-\frac{1}{1+p\varepsilon F(\alpha,\theta_b)}. \tag{41}$$

■

In Thm. 5, $\tilde{P}_{\rm di}(\theta_b)$ is in fact the standard success probability in a Poisson cellular network where interfering BSs are active independently with probability $\zeta T_{\rm f}$ [31, Eq. (29)].

2) Nearest-interferer approximation: In this system, denote by x_1 the nearest active interfering BS to the typical user. Letting $\tilde{T}_{\rm ni}$ be the packet transmission time of the typical user for cellular networks, we have the following theorem.

Theorem 6. *Given that the typical BS is active, the CCDF of $\tilde{T}_{\rm ni}$ in cellular networks is*

$$\begin{aligned}\mathbb{P}(\tilde{T}_{\rm ni}>b) = \frac{\theta_b}{1+\theta_b} - \int_0^1 \frac{x^\delta}{(1-\zeta T_{\rm f})x^\delta+\zeta T_{\rm f}} \\ \times\frac{\theta_b}{(1+\theta_b x)^2}\mathrm{d}x,\ b\le T_{\rm f}.\end{aligned} \tag{42}$$

Proof: Letting $\nu = r_0/|x_1|$, the CCDF of $\tilde{T}_{\rm ni}$ is

$$\begin{aligned}\mathbb{P}(\tilde{T}_{\rm ni}>b) &= 1-\mathbb{P}\Big(\frac{h_{x_0}\ell(x_0)}{h_{x_1}\ell(x_1)}>\theta_b\Big) \\ &= 1-\mathbb{P}\Big(\frac{h_{x_0}\nu^{-\alpha}}{h_{x_1}}>\theta_b\Big) \\ &= 1-\mathbb{E}\Big[\frac{1}{1+\theta_b\nu^\alpha}\Big] \\ &= 1-\int_0^1\frac{1}{1+\theta_b v^\alpha}\mathrm{d}\mathbb{P}(\nu<v). \end{aligned} \tag{43}$$

Next we need to derive the distribution of ν. Due to the independent thinning property, the set of active interfering BSs forms a PPP Φ'_a with density $\lambda p\varepsilon$ outside the circle centered at the origin with radius r_0. Conditioning on r_0, the distribution of $|x_1|$ is derived through calculating the probability that there is no BS belonging to Φ'_a in the ring with inner radius r_0 and outer radius $|x_1|$. Thus, we have $\mathbb{P}(|x_1|>t\mid r_0) = e^{-\lambda p\varepsilon\pi(t^2-r_0^2)}$, and the CDF of ν follows as

$$\begin{aligned}\mathbb{P}(\nu<v) &= \mathbb{P}(|x_1|>r_0/v) \\ &= \int_0^\infty e^{-\lambda p\varepsilon\pi(r^2/v^2-r^2)} f_{r_0}(r)\mathrm{d}r \\ &= \frac{v^2}{(1-p\varepsilon)v^2+p\varepsilon},\quad 0\le v\le 1. \end{aligned} \tag{44}$$

By inserting (44) into (43), the final result is obtained. ■

3) Independent-interferer approximation: In this system, each interfering BS is assumed to interfere with the typical user for an independent time duration $\tilde{T}_x$, which is identically independently distributed with $\mathbb{P}(\tilde{T}>b)$. Letting $\tilde{T}_{\rm ii}$ be the packet transmission time of the typical user in cellular networks, we obtain its CCDF as follows.

Theorem 7. *Let $\tilde{\mu}\triangleq\int_0^{T_{\rm f}}\mathbb{P}(\tilde{T}>b)\mathrm{d}b$ be the average packet transmission time of the interfering BSs in the independent-interferer system. Given that the typical BS is active, the CCDF of $\tilde{T}_{\rm ii}$ for the typical user is*

$$\tilde{P}_{\rm ii}^{\rm l}(\theta_b)\le\mathbb{P}(\tilde{T}_{\rm ii}>b)\le\tilde{P}_{\rm ii}^{\rm u}(\theta_b),\quad b\le T_{\rm f}, \tag{45}$$

where

$$\tilde{P}_{\rm ii}^{\rm u}(\theta_b) = 1-\frac{1}{1+\zeta T_{\rm f}F(\alpha,\theta_b\min\{1,\tilde{\mu}/b\})}, \tag{46}$$

$$\tilde{P}_{\rm ii}^{\rm l}(\theta_b) = 1-\frac{1}{1+\zeta\tilde{\mu}F(\alpha,\theta_b)}. \tag{47}$$

Proof: See Appendix C.

Similar to the case in Poisson bipolar networks, $\mathbb{P}(\tilde{T}>b)$ can also be chosen as the distribution of the packet transmission time in the dummy- or nearest-interferer system given in Thms. 5 and 6. Thus, $\tilde{\mu}$ can be $\tilde{\mu}_{\rm di}$ or $\tilde{\mu}_{\rm ni}$, given as follows

$$\tilde{\mu}_{\rm di} = T_{\rm f}-\int_0^{T_{\rm f}}\frac{1}{1+\zeta T_{\rm f}F(\alpha,\theta_b)}\mathrm{d}b, \tag{48}$$

$$\tilde{\mu}_{\rm ni} = \int_0^{T_{\rm f}}\frac{\theta_b\mathrm{d}b}{1+\theta_b} - \int_0^{T_{\rm f}}\int_0^1\frac{x^\delta}{(1-\zeta T_{\rm f})x^\delta+\zeta T_{\rm f}}\frac{\theta_b}{(1+\theta_b x)^2}\mathrm{d}x\mathrm{d}b. \tag{49}$$

The distribution of the packet transmission time does not depend on the scheduling probability p. The reason is that a potential transmitter becomes an interferer to the typical receiver only if $B_{x,k}=1$ and $Q_{x,k}>0$ and thus the probability of a transmitter being an interferer is $p\varepsilon=\zeta T_{\rm f}$, which is independent of p. However, such independence holds under the condition that $\zeta < p/T_{\rm f}$, i.e., the arrival rate should be less than the service rate, since, otherwise, the buffer at each transmitter is non-empty with probability 1 and p will in turn affect the CCDF of the packet transmission time.

TABLE I. Symbols and descriptions

Symbol	Description	Default value
Φ, λ	The PPP of transmitters and density	$1\times10^{-3}\,\mathrm{m}^{-2}$
α	The path loss exponent	4
T_f	The length of a frame	$1\times10^{-4}\,\mathrm{s}$
p	The scheduling probability of transmitters	0.5
r_0	The fixed distance between transmitter-receiver pair in D2D networks	$2\,\mathrm{m}$
W	The bandwidth	1 MHz
ζ	The arrival rate of the packets	400 packets/second
K	The information bits of a packet	160 bits
T_w, T	The packet waiting time, packet transmission time	N/A
μ	The average packet transmission time of interferers	N/A

VI. End-to-End Performance Analysis

In this section, to characterize the intrinsic connection between the end-to-end delay and reliability, we propose the notion of *end-to-end success probability*, which is the success probability given the end-to-end delay requirement, and use it to analyze the performance of rateless codes. To highlight the performance benefits from rateless codes, we also derive the corresponding results for fixed-rate codes.

A. The End-to-End Success Probability for Rateless Codes

The end-to-end delay D of a packet is the sum of the packet waiting time T_w and the packet transmission time T, i.e., $D = T_\mathrm{w}+T$. The CCDF of D is hence obtained through the CCDFs of T_w and T. When $b \le T_\mathrm{f}$, we have

$$\mathbb{P}(D>b) = \mathbb{P}(T_\mathrm{w}=0)\mathbb{P}(T>b) + \int_{0^+}^{b}\mathbb{P}(T>b-t)f_{T_\mathrm{w}}(t)\mathrm{d}t + \mathbb{P}(T_\mathrm{w}>b), \quad (50)$$

and when $b > T_\mathrm{f}$,

$$\mathbb{P}(D>b) = \int_{0^+}^{b}\mathbb{P}(T>b-t)f_{T_\mathrm{w}}(t)\mathrm{d}t + \mathbb{P}(T_\mathrm{w}>b), \quad (51)$$

where $f_{T_\mathrm{w}}(t)$ is the PDF of T_w. However, due to the adoption of rateless codes, the packet transmission terminates when the transmitter receives the ACK from its receiver. In this case, the transmission time of a packet can be either smaller or equal to the length of a frame T_f, and the CCDF of D cannot reflect whether the packet is successfully transmitted or not as long as the end-to-end delay is smaller than the maximum delay constraint. To jointly analyze the delay and reliability performances, we then focus on the end-to-end success probability of rateless codes in Poisson bipolar and cellular networks.

Given a delay constraint b and conditioned on $T_\mathrm{w} = t$, the success probability in the transmission phase is $1-\mathbb{P}(T > b-t)$ for $b-t < T_\mathrm{f}$ and $1-\mathbb{P}(T>T_\mathrm{f})$ for $b-t>T_\mathrm{f}$. According to the total probability law, the end-to-end success probability follows as

$$p_s(b) = \int_{0^+}^{b}\big(1-\mathbb{P}\left(T>\min\{b-t,T_\mathrm{f}\}\right)\big)f_{T_\mathrm{w}}(t)\mathrm{d}t + \mathbb{P}(T_\mathrm{w}=0)\big(1-\mathbb{P}\left(T>\min\{b,T_\mathrm{f}\}\right)\big), \quad (52)$$

where $f_{T_\mathrm{w}}(t)$ is obtained, based on the CCDF of T_w in Thm. 1, as

$$f_{T_\mathrm{w}}(t) \approx \frac{\zeta^2 T_\mathrm{f}}{p}(e^{u^*}-1)\exp\Big(-\zeta(e^{u^*}-1)(t+T_\mathrm{f})+u^*\Big),\ t>0, \quad (53)$$

and $\mathbb{P}(T>t)$ can be bounded or approximated according to Thms. 2-7.

Since the characterization of the end-to-end success probability involves multiple processes (queueing and transmission processes) and multiple metrics (packet waiting and transmission time, end-to-end delay and reliability), it is almost surely impossible to obtain closed-form analytical expressions. Although our expression involves two nested integrals, its calculation is still much more efficient than simulations.

B. The End-to-End Success Probability for Fixed-Rate Codes

When fixed-rate coding is adopted, each transmitter is active during the entire frame. Therefore, the packet transmission time is always T_f and the end-to-end delay is $D = T_\mathrm{w}+T_\mathrm{f}$. Due to the continuous transmission in each frame, the interference at the typical receiver is same as that in the dummy-interference system. Thus, the success probability ξ in the transmission phase is

$$\xi = \exp\Big(-\pi\lambda\zeta T_\mathrm{f}\Gamma(1+\delta)\Gamma(1-\delta)\theta^\delta r_0^2\Big) \quad (54)$$

for Poisson bipolar networks and

$$\xi = \frac{1}{1+\zeta T_\mathrm{f}F(\alpha,\theta)} \quad (55)$$

for Poison cellular networks, where $\theta = 2^{\frac{K}{WT_\mathrm{f}}}-1$. Hence, the end-to-end success probability of fixed-rate codes is

$$p_s(b) = \begin{cases} \xi\big(1-\mathbb{P}(T_\mathrm{w}>b-T_\mathrm{f})\big) & b\ge T_\mathrm{f} \\ 0 & b<T_\mathrm{f}. \end{cases} \quad (56)$$

VII. Numerical Results

In this section, we present numerical results that demonstrate the performance in both Poisson bipolar and cellular networks. The main symbols and parameters are summarized in Table I, and default values are given where applicable.

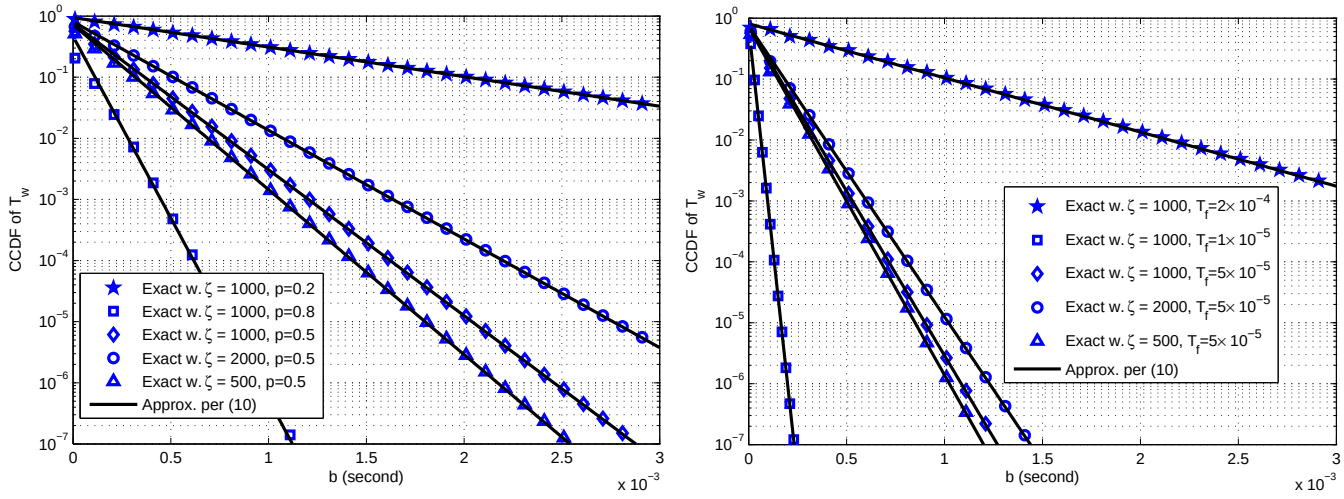

(a) The CCDF of $T_{\rm w}$ for different ζ and p.

(b) The CCDF of $T_{\rm w}$ for different ζ and $T_{\rm f}$.

Fig. 1. Validating the approximation for the CCDF of the packet waiting time.

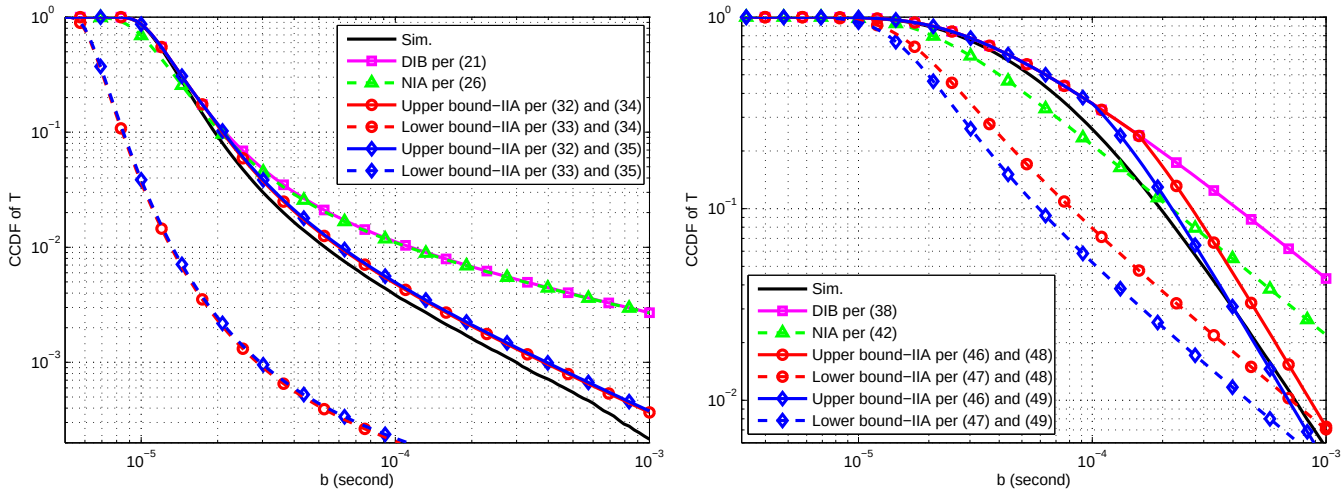

(a) The CCDF of T in Poisson bipolar networks.

(b) The CCDF of T in Poisson cellular networks.

Fig. 2. Validating the bounds and approximations for the CCDF of the packet transmission time.

A. The Distribution of the Packet Waiting Time

Fig. 1 plots the CCDFs of the packet waiting time $T_{\rm w}$ for different frame durations $T_{\rm f}$, active probabilities p and arrival rates of packets ζ, where the exact and approximative results are obtained via the inverse Laplace transform in (9) and Theorem 1, respectively. It is observed that the approximations derived from the effective bandwidth approach match the exact results extremely well under different parameter settings, which substantially enhances the analytical tractability with almost zero deviation. It is also seen that the logarithmic form of $\mathbb{P}(T_{\rm w} > b)$ decays linearly as b increases with the slope $\zeta(e^{u^*} - 1)$. Consisted with the result in (12), $\mathbb{P}(T_{\rm w} > b) \neq 1$ as $b \to 0$ since $\mathbb{P}(T_{\rm w} = 0) > 0$. In addition, the packet waiting time becomes longer as ζ or $T_{\rm f}$ increases or p decreases. The reason is that the packet waiting time depends on the queue length in the buffer, and a larger ζ will contribute to the packet backlog in the queue, while a smaller $T_{\rm f}$ or a larger p will increase the service rate and hence the packets leave the queue faster.

B. The Distribution of the Packet Transmission Time

Fig. 2 illustrates the CCDFs of the packet transmission time T with analytical bounds and approximations as well as simulation results for Poisson bipolar (in Fig. 2(a)) and cellular networks (in Fig. 2(b)). For Poisson bipolar networks, the dummy-interferer bound and the nearest-interferer approximation provide almost the same curve, which implies that the performance of the typical receiver strongly depends on the interference from the nearest transmitter. However, these two analytical results are applicable only for small transmission times, i.e., $b < 10^{-4}$, and begin to deviate from the simulation result as the transmission time increases. This is mainly due to the fact that the benefits brought by rateless codes are not considered in the dummy- and nearest-interferer systems, i.e., the phenomenon that interferers gradually cease their transmissions if they have received the ACK is not captured

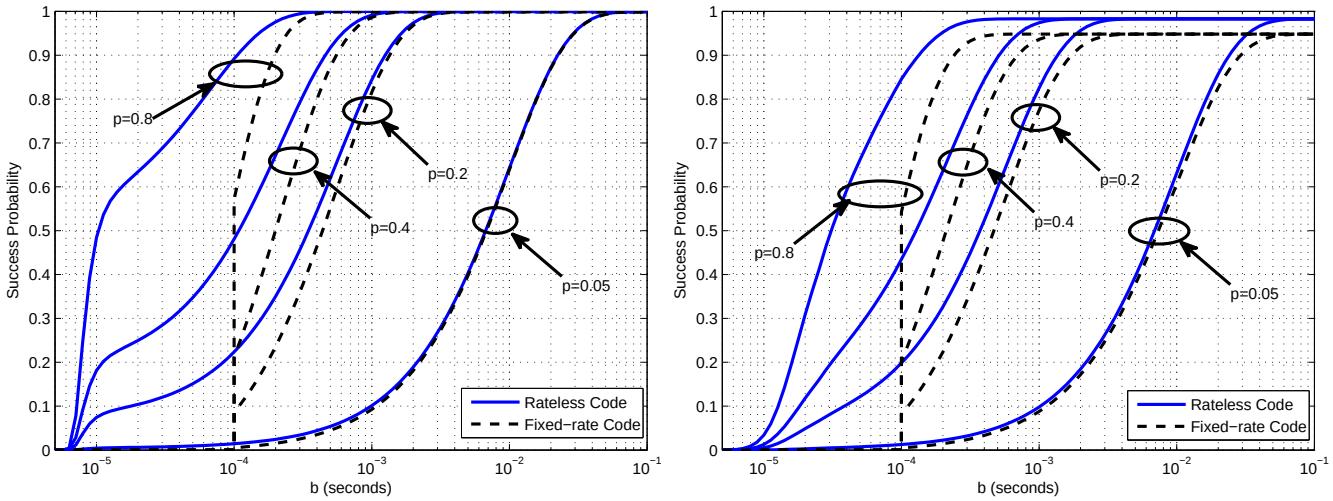

(a) Poisson bipolar networks.

(b) Poisson cellular networks.

Fig. 3. The impact of the scheduling probability on the end-to-end success probability.

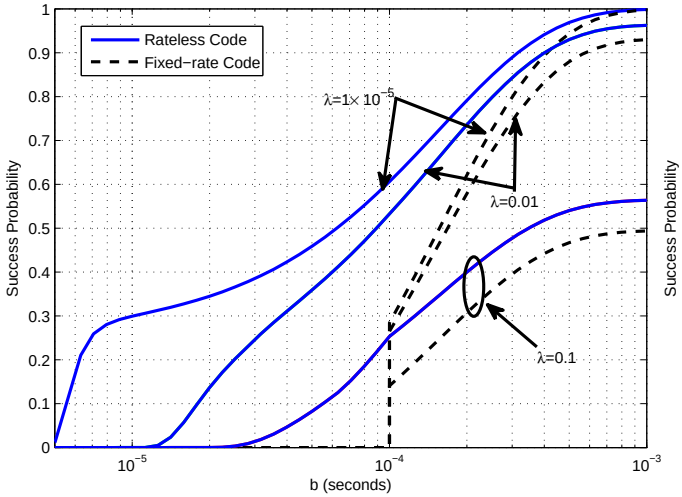

Fig. 4. The end-to-end success probability for different λ in Poisson bipolar networks with $r_0 = 5$.

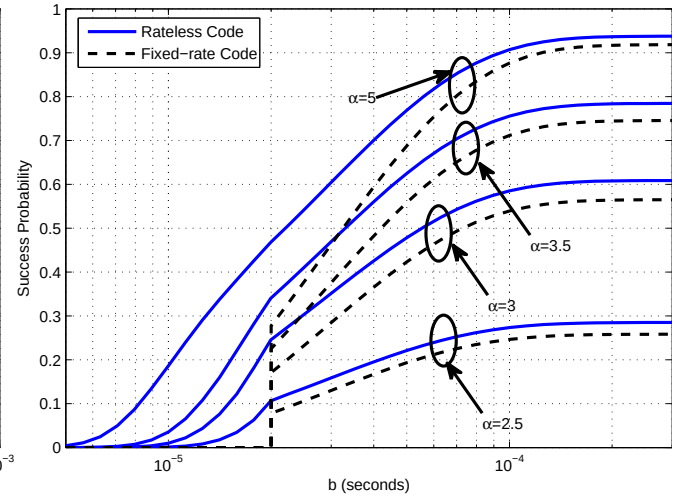

Fig. 5. The end-to-end success probability for different α in Poisson cellular networks with $T_{\mathrm{f}} = 2 \times 10^{-5}$.

by the two analytical results. Since the independent-interferer system incorporates the benefits of rateless codes, the upper bounds in this system provide the closest approximations to the simulation.

For cellular networks, the dummy-interferer bound performs similarly to that in Poisson bipolar networks while the nearest-interferer approximation has an intersection point with the simulation curve. In the early stage of each frame, the interference at the typical receiver is from all the active interfering BSs, which is equivalent to that in the dummy-interferer system and stronger than that in the nearest-interferer system. As time goes by, the interfering BSs gradually complete their transmission and stop interfering with other ongoing transmission. Thus, the interference becomes weaker than in both the dummy-interferer and nearest-interferer systems. Similarly, the upper bounds in the independent-interferer system also provide good approximations, in particular, the bound that adopts the CCDF of the packet transmission time in the nearest-interferer system is tight.

C. The End-to-End Success Probability

Due to its effectiveness, the upper bound in the independent-interferer system with the aid of NIA is used to quantify the end-to-end success probability for Poisson bipolar and cellular networks in the following.

Fig. 3 shows how the scheduling probability p affects the end-to-end success probability. It is observed that rateless coding significantly outperforms the fixed-rate coding under low delay constraints and that the performance gap between the two techniques becomes larger as p increases, which highlights the benefits of the rateless codes for delay constrained applications. When $b < T_{\mathrm{f}} = 10^{-4}$ seconds, the end-to-end success probability of fixed-rate codes is zero, because it takes a constant time of T_{f} for fixed-rate codes to perform data transmission. Moreover, for both Poisson bipolar and cellular networks, increasing p improves the end-to-end success probability due to the impact of p on the packet waiting time and the transmission time, i.e., the former reduces with the increase of p while the latter is independent of p as

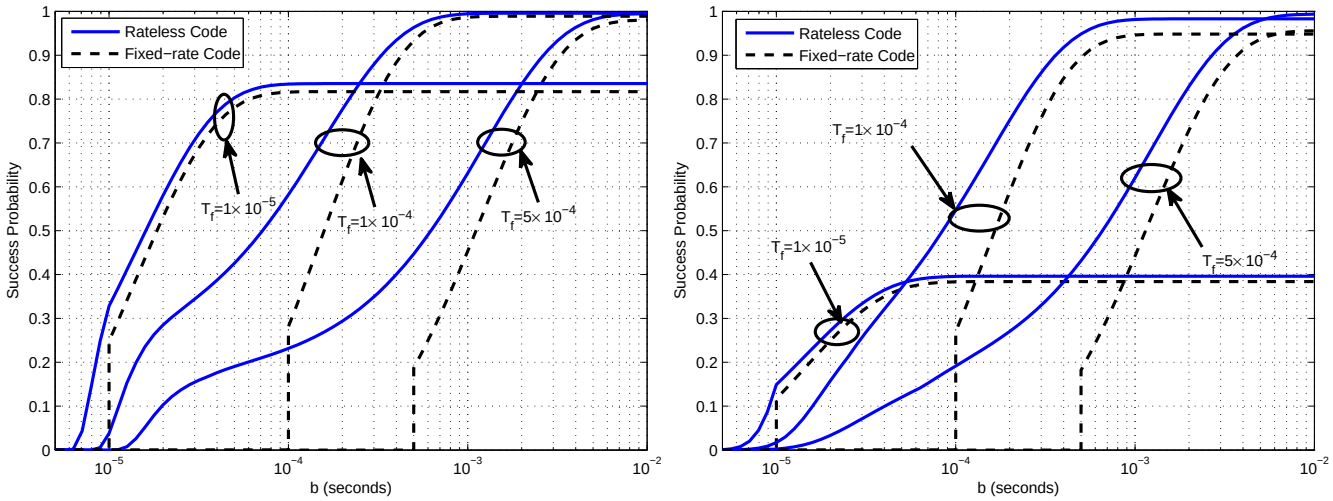

(a) Poisson bipolar networks.

(b) Poisson cellular networks

Fig. 6. The impact of the frame duration $T_{\rm f}$ on the end-to-end success probability with $\lambda = 0.01$.

long as $\zeta < p/T_{\rm f}$. When the delay constraint increases, the probability that the packet waiting time exceeds the constraint tends to 0 and the end-to-end success probability is dominated by whether the packet is successfully transmitted.

Since p only affects the packet waiting time while λ and α merely affect the transmission time, we next study the impacts of λ and α on the end-to-end success probability in Poisson bipolar and cellular networks, respectively, in Figs. 4 and 5. It is seen in Fig. 4 that a smaller density leads to a better end-to-end success probability and a larger performance gap between rateless and fixed-rate codes. Furthermore, the packet can be successfully transmitted in a shorter time using rateless codes in the case with smaller density and hence the constraint for the packet waiting time can be relaxed more, which means that the end-to-end transmission can still succeed even if the packet waiting time is larger than $b - T_{\rm f}$. However, if fixed-rate codes are adopted, the constraint for the packet waiting time is constant as $b - T_{\rm f}$ for different densities. Fig. 5 shows that a larger path loss exponent leads to a better end-to-end success probability and larger performance gap between the two coding schemes. Due to the nearest-BS association, a larger α leads to more severe power attenuation for the interfering signals than the desired signal, and thus improves the success probability. The two figures reveal the positive correlation between the packet waiting time and transmission time by means of rateless codes, i.e., the reduction of either side will relax the requirement of the other, which does not hold for fixed-rate codes.

Fig. 6 shows the impact of the frame duration $T_{\rm f}$ on the end-to-end success probability, where $T_{\rm f}$ affects both waiting and transmission time of a packet. For different $T_{\rm f}$, rateless codes achieve better performance than fixed-rate codes. As for the impact of $T_{\rm f}$ on the performance, we can see that under an extremely strict delay requirement, a smaller value of $T_{\rm f}$ (e.g., $T_{\rm f} = 1 \times 10^{-5}$) is superior to a larger one (e.g., $T_{\rm f} = 1 \times 10^{-4}, 5 \times 10^{-4}$) in terms of the end-to-end success probability. Thus, in this case, one should try to increase the success probability of a single transmission, e.g., by adopting rateless codes rather than fixed-rate codes. In contrast, when the delay constraint becomes loose, the plateau of the success probability is higher with a larger $T_{\rm f}$ due to the fact that it is more likely to successfully transmit a fixed-size information packet over a longer frame. Therefore, there are two key tradeoffs: one is between the transmission reliability and the delay requirement; and the other is between the packet waiting time and the packet transmission time under an end-to-end delay requirement, both of which require a judicious choice of the frame duration. Besides, the smaller $T_{\rm f}$, the faster the probability of the packet waiting time exceeding the delay constraint tends to zero, and hence the earlier entry into the plateau for the success probability.

VIII. Conclusions

In this paper, we proposed a general framework for the end-to-end performance analysis of rateless codes in Poisson bipolar and cellular networks where both the spatial distribution of transmitters and traffic dynamics are incorporated. We first investigated the end-to-end delay through dividing it into two parts, namely, the packet waiting time and transmission time, and then provided analytical results including bounds and approximations for their statistical distributions. Through comparison with Monte Carlo simulations, we validated that our proposed approximations match the actual distributions well. Interestingly, the scheduling probability merely affects the packet waiting time if the arrival rate is smaller than the service rate.

Furthermore, we derived the end-to-end success probability, defined as the probability of successful transmission within an end-to-end delay constraint, through the tractable yet accurate approximations for the packet waiting and transmission time, which characterizes the delay and reliability performance jointly. The results reveal that the parameters such as the scheduling probability, the network density, and the path loss exponent affect either the packet waiting time or transmission

time and present monotonic effects on the end-to-end success probability, while the frame duration plays a critical role in balancing the tradeoff between the transmission reliability and the delay requirement. In addition, the frame duration also serves as a regulator between the packet waiting time and the packet transmission time under an end-to-end delay constraint, which, in turn, affects the end-to-end success probability. The full comparison shows the significant benefits of rateless codes relative to the fixed-rate codes in terms of the end-to-end reliability and delay, which indicates that rateless coding offers great potential to achieve the stringent requirement of future emerging applications, e.g., the URLLC scenario, possibly in combination with other technologies like mm-wave communication, massive MIMO, ultra-dense networks or coordinated multi-point transmissions.

Appendix A
Proof of Theorem 1

Proof: Using the effective bandwidth and capacity in [24, 25], the distributions of the steady-state queue length $Q(\infty)$ and the queueing delay $D_{\rm q}(\infty)$ can be asymptotically characterized and accurately approximated. Denote by $A(t)$ and $S(t)$ the total number of packets reaching and leaving the buffer in t time instants, respectively. We first obtain the asymptotic log-moment generating functions of the arrival and service processes, respectively, given by

$$\begin{aligned}\Lambda_A(u) &= \lim_{t\to\infty}\frac{1}{t}\log\mathbb{E}\left[e^{uA(t)}\right]\\ &= \lim_{t\to\infty}\frac{1}{t}\log\left(\sum_{n=0}^{\infty}e^{un}e^{-\zeta t}\frac{(\zeta t)^n}{n!}\right)\\ &= \zeta(e^u-1),\end{aligned}\tag{57}$$

and

$$\begin{aligned}\Lambda_S(u) &= \lim_{N\to\infty}\frac{1}{NT_{\rm f}}\log\mathbb{E}\left[e^{uS(NT_{\rm f})}\right]\\ &= \lim_{N\to\infty}\frac{1}{NT_{\rm f}}\log\left(\sum_{n=0}^{N}e^{un}\binom{N}{n}p^n(1-p)^{N-n}\right)\\ &= \frac{1}{T_{\rm f}}\log(pe^u+1-p).\end{aligned}\tag{58}$$

Then, the effective bandwidth of the arrival process is $E(u)=\Lambda_A(u)/u$. Accordingly, the violation probabilities of the steady-state queueing length and the queueing delay under small threshold can be accurately approximated by

$$\begin{aligned}&\mathbb{P}(Q(\infty)>Q_{\rm th})\approx\mathbb{P}(Q(\infty)>0)\exp(-u^*Q_{\rm th}),\\ &\mathbb{P}(D_{\rm q}(\infty)>D_{\rm th})\approx\mathbb{P}(Q(\infty)>0)\exp(-u^*E(u^*)D_{\rm th}),\end{aligned}\tag{59}$$

where $\mathbb{P}(Q(\infty)>0)=\zeta T_{\rm f}/p$ is the probability that the buffer is not empty, and $u^*>0$ is the decay rate of the tail distribution of the queue length, satisfying $\Lambda_A(u^*)+\Lambda_S(-u^*)=0$. From (59), these two violation probabilities are equivalent by letting $Q_{\rm th}=E(u^*)D_{\rm th}$.

For a given packet, its sojourn time is its queueing delay in the buffer plus its service time, which is equivalent to the queueing delay of a packet with an extra one before it. Therefore, the CCDF of the packet waiting time is

$$\begin{aligned}\mathbb{P}(T_{\rm w}>b) &= \mathbb{P}(T_{\rm sj}>b+T_{\rm f})\\ &\approx \mathbb{P}(Q(\infty)+1>(b+T_{\rm f})E(u^*))\\ &\approx \frac{\zeta T_{\rm f}}{p}\exp\big(-u^*(b+T_{\rm f})E(u^*)+u^*\big).\end{aligned}\tag{60}$$

■

Appendix B
Proof of Theorem 4

Proof: According to (30), we have

$$\begin{aligned}\mathbb{P}(T_{\rm ii}>b) &= \mathbb{P}\Big(K>bW\log_2\Big(1+\frac{h_{x_0}\ell(x_0)}{\bar{I}(b)}\Big)\Big)\\ &= 1-\mathbb{P}\Big(\frac{h_{x_0}\ell(x_0)}{\bar{I}(b)}>\theta_b\Big)\\ &= 1-\mathcal{L}_{\bar{I}(b)}(\theta_b r_0^{\alpha}).\end{aligned}\tag{61}$$

Similar to the derivation of $\mathcal{L}_{I_{\rm di}}$, the Laplace transform of $\bar{I}(b)$ is

$$\begin{aligned}\mathcal{L}_{\bar{I}(b)}(s) &= \mathbb{E}[e^{-s\bar{I}(b)}]\\ &= \mathbb{E}\Big[\prod_{x\in\Phi'}\Big(1-p\varepsilon+p\varepsilon e^{-s\ell(x)h_x\bar{\eta}_x(b)}\Big)\Big]\\ &= \exp\Big(-2\pi\lambda p\varepsilon\int_0^{\infty}\mathbb{E}_{h,\bar{\eta}(t)}\big[1-e^{-sh\bar{\eta}(b)r^{-\alpha}}\big]r{\rm d}r\Big)\\ &= \exp\Big(-\pi\lambda p\varepsilon\mathbb{E}(\bar{\eta}(b)^{\delta})\Gamma(1+\delta)\Gamma(1-\delta)s^{\delta}\Big),\end{aligned}\tag{62}$$

where $\mathbb{E}(\bar{\eta}(b)^{\delta})$ performs the expectation over the packet transmission time $\bar{T}$ of the interfering transmitters. By inserting $\mathcal{L}_{\bar{I}(b)}$ into (61), we have

$$\mathbb{P}(T_{\rm ii}>b)=1-\exp\Big(-\pi\lambda p\varepsilon\mathbb{E}(\bar{\eta}(b)^{\delta})\Gamma(1+\delta)\Gamma(1-\delta)\theta_b^{\delta}r_0^2\Big).\tag{63}$$

For notational simplicity, we define $g(\bar{T})=\big[\min\{1,\bar{T}/b\}\big]^{\delta}$, and thus we have $\mathbb{E}(\bar{\eta}(b)^{\delta})=\mathbb{E}[g(\bar{T})]$. The concavity of $g(\bar{T})$ can be verified easily by its 2nd derivative

$$\frac{{\rm d}^2g(\bar{T})}{{\rm d}^2\bar{T}}=\begin{cases}\delta(\delta-1)\bar{T}^{\delta-2}/b^{\delta} & \bar{T}\le b\\ 0 & b<\bar{T}\le T_{\rm f},\end{cases}\tag{64}$$

which shows that $g^{(2)}(\bar{T})\le 0$ for $\bar{T}\in[0,T_{\rm f}]$. Hence, we have $\mathbb{E}[g(\bar{T})]\le g(\mathbb{E}(\bar{T}))=\big[\min\{1,\mu/b\}\big]^{\delta}$ and $\mathbb{E}[g(\bar{T})]\ge\mu/T_{\rm f}$ due to

$$g(\bar{T})\ge\Big(1-\frac{\bar{T}}{T_{\rm f}}\Big)g(0)+\frac{\bar{T}}{T_{\rm f}}g(T_{\rm f})=\frac{\bar{T}}{T_{\rm f}}.\tag{65}$$

The final results are obtained by substituting the two bounds of $\mathbb{E}[g(\bar{T})]$ in (63). ■

Appendix C
Proof of Theorem 7

Proof: From (36),

$$\mathbb{P}(\tilde{T}_{\rm ii}>b)=1-\int_0^{\infty}\mathcal{L}_{\bar{I}(b)}(\theta_b r^{\alpha})f_{r_0}(r){\rm d}r,\tag{66}$$

where

$$\tilde{I}(b) = \sum_{x\in\Phi'} \ell(x) h_x B_x \mathbf{1}_{Q_x>0} \tilde{\eta}_x(b),\ 0 < b \le T_{\rm f}, \tag{67}$$

and $\tilde{\eta}_x(b) = \min\{1, \tilde{T}_x/b\}$. Given that $r_0 = r$, the Laplace transform of $\tilde{I}(b)$ in cellular networks evaluated at $s = \theta_b r^\alpha$ is

$$\begin{aligned}\mathcal{L}_{\tilde{I}(b)}(\theta_b r^\alpha) &= \mathbb{E}\Big[\exp\big(-\theta_b r^\alpha \sum_{x\in\Phi'} \ell(x) h_x B_x \mathbf{1}_{Q_x>0}\tilde{\eta}_x(b)\big)\Big] \\ &= \mathbb{E}\Big[\prod_{x\in\Phi'}\Big(1 - p\varepsilon + \frac{p\varepsilon}{1+\theta_b r^\alpha |x|^{-\alpha}\tilde{\eta}_x(b)}\Big)\Big] \\ &= \exp\Big(-2\pi\lambda p\varepsilon \mathbb{E}\Big[\int_r^\infty \frac{\theta_b (\frac{r}{t})^\alpha \tilde{\eta}(b)}{1+\theta_b(\frac{r}{t})^\alpha\tilde{\eta}(b)} t{\rm d}t\Big]\Big), \end{aligned} \tag{68}$$

where $\mathbb{E}$ in the last step performs expectation over $\tilde{T}$ due to $\tilde{\eta}(b) = \min\{1, \tilde{T}/b\}$. For notational simplicity, letting $\varpi = \theta_b r^\alpha t^{-\alpha}$, we define $z(\tilde{T}) = \frac{1}{1+\varpi\min\{1,\tilde{T}/b\}}$ and its 2nd derivative is

$$\frac{{\rm d}^2 z(\tilde{T})}{{\rm d}^2\tilde{T}} = \begin{cases} \frac{2(\varpi/b)^2}{(1+\varpi\tilde{T}/b)^3} & \tilde{T} \le b \\ 0 & b < \tilde{T} \le T_{\rm f}, \end{cases} \tag{69}$$

Thus $z(\tilde{T})$ is a convex function due to $z^{(2)}(\tilde{T}) \ge 0$ for $\tilde{T} \in [0, T_{\rm f}]$. Then, we have $\mathbb{E}[z(\tilde{T})] \ge z(\mathbb{E}(\tilde{T})) = z(\tilde{\mu})$, and $\mathcal{L}_{\tilde{I}(b)}(\theta_b r^\alpha)$ is lower bounded as

$$\begin{aligned}\mathcal{L}_{\tilde{I}(b)}(\theta_b r^\alpha) &\ge \exp\Big(-2\pi\lambda p\varepsilon \int_r^\infty \frac{\theta_b (r/t)^\alpha \min\{1, \frac{\tilde{\mu}}{b}\}}{1+\theta_b(r/t)^\alpha \min\{1,\frac{\tilde{\mu}}{b}\}} t{\rm d}t\Big) \\ &\overset{(a)}{=} \exp\Big(-\pi\lambda p\varepsilon r^2 F(\alpha, \theta_b \min\{1, \tilde{\mu}/b\})\Big), \end{aligned} \tag{70}$$

where step (a) follows from the same derivation as (39). Due to the convexity of $z(\tilde{T})$, it is lower bounded as

$$\begin{aligned} z(\tilde{T}) &\le \Big(1 - \frac{\tilde{T}}{T_{\rm f}}\Big) z(0) + \frac{\tilde{T}}{T_{\rm f}} z(T_{\rm f}) \\ &= 1 - \frac{\tilde{T}}{T_{\rm f}} + \frac{\tilde{T}}{T_{\rm f}} \frac{1}{1+\varpi}. \end{aligned} \tag{71}$$

Thus, $\mathbb{E}[z(\tilde{T})] \le 1 - \frac{\tilde{\mu}}{T_{\rm f}} + \frac{\tilde{\mu}}{T_{\rm f}}\frac{1}{1+\varpi}$ and $\mathcal{L}_{\tilde{I}(b)}(\theta_b r^\alpha)$ is upper bounded as

$$\begin{aligned}\mathcal{L}_{\tilde{I}(b)}(\theta_b r^\alpha) &\le \exp\Big(-2\pi\lambda p\varepsilon \frac{\tilde{\mu}}{T_{\rm f}} \int_r^\infty \Big(1 - \frac{1}{1+\theta_b r^\alpha t^{-\alpha}}\Big) t{\rm d}t\Big) \\ &= \exp\Big(-\pi\lambda p\varepsilon \frac{\tilde{\mu}}{T_{\rm f}} r^2 F(\alpha, \theta_b)\Big). \end{aligned} \tag{72}$$

By substituting (71) and (72) in (66), the final results are obtained. ∎

REFERENCES

[1] N. Deng and M. Haenggi, "Delay characterization of rateless codes in wireless ad hoc networks," in *IEEE International Conference on Communications (ICC'19)*, Shanghai, China, May 2019.

[2] A. Osseiran, F. Boccardi, V. Braun *et al.*, "Scenarios for 5G mobile and wireless communications: the vision of the METIS project," *IEEE Communications Magazine*, vol. 52, no. 5, pp. 26–35, May 2014.

[3] D. P. Bertsekas and R. G. Gallager, *Data Networks (Second Edition)*. Prentice Hall, 1992.

[4] Y. Zhong, M. Haenggi, F. Zheng, W. Zhang, T. Q. S. Quek, and W. Nie, "Toward a tractable delay analysis in ultra-dense networks," *IEEE Communications Magazine*, vol. 55, no. 12, pp. 103–109, Dec. 2017.

[5] 3GPP, "Study on scenarios and requirements for next generation access technologies," 3rd Generation Partnership Project (3GPP), Technical Report (TR) 38.913, Jun. 2018, version 15.0.0.

[6] N. Bonello, Y. Yang, S. Aissa, and L. Hanzo, "Myths and realities of rateless coding," *IEEE Communications Magazine*, vol. 49, no. 8, pp. 143–151, Aug. 2011.

[7] J. Castura and Y. Mao, "Rateless coding and relay networks," *IEEE Signal Processing Magazine*, vol. 24, no. 5, pp. 27–35, Sept. 2007.

[8] J. Castura, Y. Mao, and S. Draper, "On rateless coding over fading channels with delay constraints," in *2006 IEEE International Symposium on Information Theory*, Jul. 2006, pp. 1124–1128.

[9] M. Hashemi, Y. Cassuto, and A. Trachtenberg, "Fountain codes with nonuniform selection distributions through feedback," *IEEE Transactions on Information Theory*, vol. 62, no. 7, pp. 4054–4070, Jul. 2016.

[10] H. ElSawy, E. Hossain, and M. Haenggi, "Stochastic geometry for modeling, analysis, and design of multi-tier and cognitive cellular wireless networks: A survey," *IEEE Communications Surveys Tutorials*, vol. 15, no. 3, pp. 996–1019, Third quarter 2013.

[11] H. ElSawy, A. Sultan-Salem, M. Alouini, and M. Z. Win, "Modeling and analysis of cellular networks using stochastic geometry: A tutorial," *IEEE Communications Surveys Tutorials*, vol. 19, no. 1, pp. 167–203, First quarter 2017.

[12] M. Haenggi, *Stochastic geometry for wireless networks*. Cambridge University Press, 2012.

[13] K. Stamatiou and M. Haenggi, "Random-access Poisson networks: Stability and delay," *IEEE Communications Letters*, vol. 14, no. 11, pp. 1035–1037, Nov. 2010.

[14] ——, "Delay characterization of multihop transmission in a Poisson field of interference," *IEEE/ACM Transactions on Networking*, vol. 22, no. 6, pp. 1794–1807, Dec. 2014.

[15] Y. Zhong, T. Q. S. Quek, and X. Ge, "Heterogeneous cellular networks with spatio-temporal traffic: Delay analysis and scheduling," *IEEE Journal on Selected Areas in Communications*, vol. 35, no. 6, pp. 1373–1386, Jun. 2017.

[16] A. F. Molisch, N. B. Mehta, J. S. Yedidia, and J. Zhang, "Performance of fountain codes in collaborative relay networks," *IEEE Transactions on Wireless Communications*, vol. 6, no. 11, pp. 4108–4119, Nov. 2007.

[17] K. Pang, Z. Lin, B. F. Uchoa-Filho, and B. Vucetic, "Distributed network coding for wireless sensor networks based on rateless LT codes," *IEEE Wireless Communications Letters*, vol. 1, no. 6, pp. 561–564, Dec. 2012.

[18] C. Stefanovic and P. Popovski, "ALOHA random access that operates as a rateless code," *IEEE Transactions on Communications*, vol. 61, no. 11, pp. 4653–4662, Nov. 2013.

[19] R. Diamant and L. Lampe, "Adaptive error-correction coding scheme for underwater acoustic communication networks," *IEEE Journal of Oceanic Engineering*, vol. 40, no. 1, pp. 104–114, Jan. 2015.

[20] X. Di, K. Xiong, P. Fan, and H. Yang, "Simultaneous wireless information and power transfer in cooperative relay networks with rateless codes," *IEEE Transactions on Vehicular Technology*, vol. 66, no. 4, pp. 2981–2996, Apr. 2017.

[21] A. Rajanna, I. Bergel, and M. Kaveh, "Performance analysis of rateless codes in an ALOHA wireless ad hoc network," *IEEE Transactions on Wireless Communications*, vol. 14, no. 11, pp. 6216–6229, Nov. 2015.

[22] A. Rajanna and M. Haenggi, "Enhanced cellular coverage and throughput using rateless codes," *IEEE Transactions on Communications*, vol. 65, no. 5, pp. 1899–1912, May 2017.

[23] J. N. Daigle, *Queueing theory with applications to packet telecommunication*. Springer Science & Business Media, 2005.

[24] D. Wu and R. Negi, "Effective capacity: a wireless link model for support of quality of service," *IEEE Transactions on Wireless Communications*, vol. 2, no. 4, pp. 630–643, Jul. 2003.

[25] S. Akin and M. Fidler, "A method for cross-layer analysis of transmit buffer delays in message index domain," *IEEE Transactions on Vehicular Technology*, vol. 67, no. 3, pp. 2698–2712, Mar. 2018.

[26] 3GPP, "Evolved Universal Terrestrial Radio Access (E-UTRA) Physical channels and modulation," 3rd Generation Partnership Project (3GPP), Technical Specification (TS) 36.211, March 2019, version 15.5.0.

[27] A. Lapidoth, "Nearest neighbor decoding for additive non-Gaussian noise channels," *IEEE Transactions on Information Theory*, vol. 42, no. 5, pp. 1520–1529, Sept. 1996.

[28] Y. Polyanskiy, H. V. Poor, and S. Verdu, "Channel coding rate in the finite blocklength regime," *IEEE Transactions on Information Theory*, vol. 56, no. 5, pp. 2307–2359, May 2010.

[29] M. Haenggi, "On distances in uniformly random networks," *IEEE Transactions on Information Theory*, vol. 51, no. 10, pp. 3584–3586, Oct. 2005.
[30] X. Zhang and M. Haenggi, "A stochastic geometry analysis of inter-cell interference coordination and intra-cell diversity," *IEEE Transactions on Wireless Communications*, vol. 13, no. 12, pp. 6655–6669, Dec. 2014.
[31] M. Haenggi, "The meta distribution of the SIR in Poisson bipolar and cellular networks," *IEEE Transactions on Wireless Communications*, vol. 15, no. 4, pp. 2577–2589, Apr. 2016.

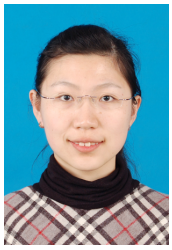

Na Deng (S'12-M'17) received the Ph.D. and B.S. degrees in information and communication engineering from the University of Science and Technology of China (USTC), Hefei, China, in 2015 and 2010, respectively. Currently she is an Associate Professor at Dalian University of Technology, Dalian, China. In 2013-2014, she was a Visiting Student in Prof. Martin Haenggi's group at the University of Notre Dame, Notre Dame, IN, USA, and in 2015-2016 she was a Senior Engineer at Huawei Technologies Co., Ltd., Shanghai, China. Her scientific interests include networking and wireless communications, green communications, and network design based on wireless big data.

Martin Haenggi (S'95-M'99-SM'04-F'14) received the Dipl.-Ing. (M.Sc.) and Dr.sc.techn. (Ph.D.) degrees in electrical engineering from the Swiss Federal Institute of Technology in Zurich (ETH) in 1995 and 1999, respectively. Currently he is the Freimann Professor of Electrical Engineering and a Concurrent Professor of Applied and Computational Mathematics and Statistics at the University of Notre Dame, Indiana, USA. In 2007-2008, he was a visiting professor at the University of California at San Diego, and in 2014-2015 he was an Invited Professor at EPFL, Switzerland. He is a co-author of the monographs "Interference in Large Wireless Network" (NOW Publishers, 2009) and "Stochastic Geometry Analysis of Cellular Networks" (Cambridge University Press, 2018) and the author of the textbook "Stochastic Geometry for Wireless Networks" (Cambridge, 2012), and he published 15 single-author journal articles. His scientific interests lie in networking and wireless communications, with an emphasis on cellular, amorphous, ad hoc (including D2D and M2M), cognitive, and vehicular networks. He served as an Associate Editor of the Elsevier Journal of Ad Hoc Networks, the IEEE Transactions on Mobile Computing (TMC), the ACM Transactions on Sensor Networks, as a Guest Editor for the IEEE Journal on Selected Areas in Communications, the IEEE Transactions on Vehicular Technology, and the EURASIP Journal on Wireless Communications and Networking, as a Steering Committee member of the TMC, and as the Chair of the Executive Editorial Committee of the IEEE Transactions on Wireless Communications (TWC). From 2017 to 2018, he was the Editor-in-Chief of the TWC. He also served as a Distinguished Lecturer for the IEEE Circuits and Systems Society, as a TPC Co-chair of the Communication Theory Symposium of the 2012 IEEE International Conference on Communications (ICC'12), of the 2014 International Conference on Wireless Communications and Signal Processing (WCSP'14), and the 2016 International Symposium on Wireless Personal Multimedia Communications (WPMC'16). For both his M.Sc. and Ph.D. theses, he was awarded the ETH medal. He also received a CAREER award from the U.S. National Science Foundation in 2005 and three awards from the IEEE Communications Society, the 2010 Best Tutorial Paper award, the 2017 Stephen O. Rice Prize paper award, and the 2017 Best Survey paper award, and he is a 2017 and 2018 Clarivate Analytics Highly Cited Researcher.